Solidly Mounted Resonators Based on ZnO/SiO_2 Acoustic Reflectors and Their Performance After High-temperature Exposure

José Manuel Carmona Cejas, Teona Mirea, Marta Clement and Jimena Olivares
GMME-CEMDATIC-ETSIT
Universidad Politécnica de Madrid
Madrid, Spain
jm.carmona@upm.es

***Abstract*— Solidly mounted resonators (SMRs) built on dielectric acoustic reflectors can save several fabrication steps as well as avoid undesired parasitic effects when exciting extended electrodes via capacitive coupling. In this work we manufacture and measure the frequency response of AlN-based SMRs built on 7-layer ZnO/SiO_2 acoustic reflectors with SiO_2 working as low impedance material and ZnO as high impedance material. After applying a 700ºC treatment, their frequency response is measured again and compared with the pre-treatment measurements.**

Keywords— Acoustic reflectors, Bragg mirrors, dielectric materials, SMRs, BAW, electrical insulators, ZnO, AlN, piezoelectric devices.

I. Introduction

Good acoustic isolation is needed to improve the performance of film bulk acoustic resonators (FBARs), either by fabricating them in free-standing configuration or on top of acoustic reflectors. Free-standing configurations are usually the ones providing better confinement of acoustic energy. However, these devices are quite fragile as well as demanding and delicate in terms of manufacture [1]. Considering this, solidly mounted resonators (SMRs) based on acoustic reflectors are the preferred choice when more rugged and less pressure sensitive devices are needed. Thus, designing and fabricating acoustic reflectors capable of providing good acoustic insulation to the piezoelectric slab have been always a key process step in SMRs.

An acoustic reflector is often made of alternated layers of high and low acoustic impedance materials, being SiO_2 the most common low impedance material as it presents proper acoustic characteristics, as well established within the industry. Metallic materials such as W [2], Ir [3] and Mo [4] are usually the ones occupying the high impedance material position, but they are prone to generate undesired capacitive coupling effects if specific configurations for the grounding electrode, are used [2]. Accessing the bottom electrode by capacitive coupling avoids the use of additional masking steps and etching through the AlN piezoelectric layer. A structure based on capacitive coupling and extended electrode is shown in fig. 1. The extension of the top electrode is employed in specific setups where we need to separate the active resonating area from the pure electrical pad. In this case, the bottom electrode must be etched below the electrical pad to prevent the appearance of parallel resonators. Even if the bottom electrode is etched below the electrical pad, if the acoustic reflector has metallic layers, capacitive coupling and generation of a parallel resonator can still happen. To avoid this, fully non-conductive acoustic reflectors are mandatory. Different non-conductive high acoustic impedance materials have been studied, as SiN, AlN [5], Ta_2O_5 [6] or HfO_2 [7]. However, SMRs based on these acoustic reflectors have not reached the performances that reflectors with metallic layers can achieve. A specific application of these fully non-conductive reflectors is of special interest, namely at very high temperatures. SMRs can be employed as gravimetric gas sensors in harsh environments due to their advantages compared to the typically studied SAW devices: they can be designed with thicker electrodes, which overcomes the power and destructive limitations of interdigital transducers (IDTs).

Here we show how an acoustic reflector made of ZnO, working as high impedance layer, and SiO_2 as low impedance layer, can provide a good acoustic confinement tool for AlN-based resonators, as previously presented [8]. Additionally, we test their behavior under high temperatures. Longitudinal mode devices and shear mode devices have been monitored both at room temperature and after a 700ºC treatment in vacuum, proving the viability of ZnO/SiO_2 acoustic reflectors under harsh circumstances.

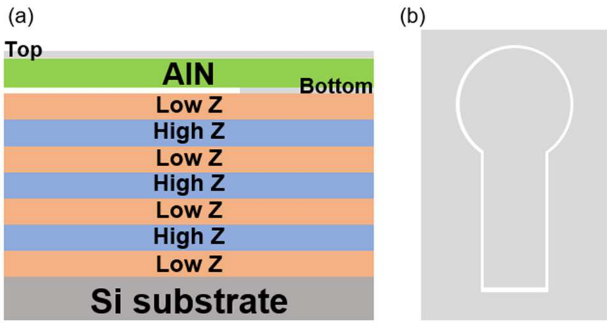

Fig. 1. (a) SMR on acoustic reflector diagram. Bottom electrode is not reachable directly by RF probe and is excited by capacitive coupling. (b) Top view diagram of an SMR with patterned top electrode extension.

II. FABRICATION PROCESS

ZnO/SiO_2 acoustic reflectors were made via DC-pulsed sputtering on 4-inch Si wafers, consisting in 7 alternated 510 nm-thick SiO_2 and 506 nm-thick ZnO layers. Reflector design was carried out by Mason's model simulations, taking care of the thicknesses of each thin film. To test their acoustic insulation properties, two types of AlN-based SMRs were grown on top of them: c-axis oriented AlN layers were grown to have longitudinal mode devices and tilted AlN layers were grown to obtain shear mode devices. Both SMRs had a Mo layer working as top electrode, patterned via photolithography, and an Ir layer intended to work as bottom electrode. Then, these SMRs built on the fully-dielectric acoustic reflectors were characterized measuring their piezoelectric response to be able to see how good the acoustic insulation provided by the reflectors is.

III. EXPERIMENTAL CHARACTERIZATION

To test the thermal stability of ZnO working as high impedance material, the SMRs described in the previous section were exposed to a thermal treatment of 700ºC in 10^{-6} mTorr vacuum for 2 hours. After that, frequency response was assessed for the different devices using a network analyzer by measuring their S11 parameters. Their acoustic properties were calculated and analyzed together with the ones obtained before the treatment.

Fig. 2 shows the longitudinal mode frequency response evaluated before and after applying the thermal treatment. From this graph one can observe that the thermal treatment probably induces a higher degradation of the resonant mode compared to the antiresonant one, although it could also be an effect of the RF probe used for the measurements. On fig. 3 the shear mode frequency response can be observed. In this case no extra signs of degradation are identifiable after high temperature exposure, meaning that acoustic reflector remains stable and brings no extra sources of energy loss. However, a good number of spurious modes are observed both before and after the thermal treatment. These undesired modes could come from different sources, from the topology of the device to the reflector itself. Specific techniques could be applied to reduce their presence.

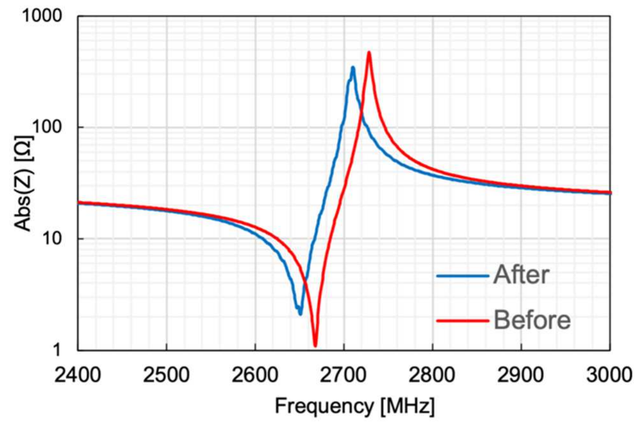

Fig. 2. Frequency response before and after 700ºC exposition, displaying the behavior of the longitudinal mode of the c-axis oriented AlN SMRs on ZnO/SiO_2 reflectors.

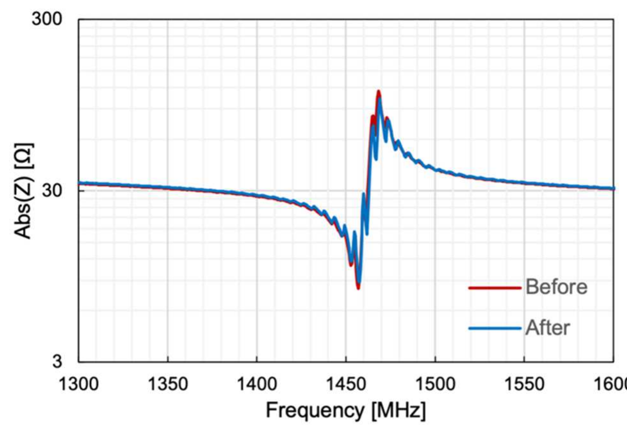

Fig. 3. Frequency response before and after 700ºC exposition showing the behavior of the shear mode of the tilted AlN SMRs on ZnO/SiO_2 reflectors.

From the measurements shown in fig. 2 and fig. 3 some important parameters related to piezoelectric activity and acoustic insulation were worked out. Electromechanical coupling coefficient (k_{eff}^2) was obtained following the formula

$$k_{eff}^2 = 100\frac{\pi f_r}{2f_a \tan[\frac{\pi f_r}{2f_a}]} \quad (1)$$

where f_r is the resonant frequency and f_a is the antiresonant frequency. Q factors were also obtained following the formula

$$Q_i = 0.5 f_i \frac{d\phi(f)}{df}\Big|_{f=f_i} \quad i = r, a \quad (2)$$

where ϕ is the phase of the impedance Z. The results are shown in table I, where the mean values for each parameter are gathered for more than 5 measurements with the uncertainty being of one standard deviation. Frequency and k_{eff}^2 values show almost no variation, meaning that piezoelectric properties remain stable after high temperature exposure and no harm has been caused to the AlN layer. Regarding Q factor values, Q_a values remain quite similar for longitudinal mode, while Q_r seems to experience some degradation, as could be glimpsed from fig. 2. For the shear mode, both Q_r and Q_a show slightly better values after 700ºC exposure, thus making it clear that no extra acoustic energy loss mechanism has appeared, and the acoustic reflector does not show any sign of degradation.

TABLE I. CHARACTERIZATION RESULTS

		f_r (GHz)	f_a (GHz)	k_{eff}^2 (%)	Q_r	Q_a
Long. Mode	**Before 700ºC**	2.66±0.01	2.73±0.01	5.4±0.2	476±151	440±137
	After 700ºC	2.65±0.01	2.71±0.01	5.3±0.2	360±74	454±60
Shear Mode	**Before 700ºC**	1.48±0.04	1.49±0.04	1.6±0.3	351±55	299±80
	After 700ºC	1.49±0.04	1.50±0.05	1.9±0.6	420±115	339±108

Temperature coefficient of frequency (TCF) measurements were also carried out for resonant and antiresonant frequencies from both longitudinal and shear modes. To calculate TCFs, these frequencies were obtained at temperatures ranging from 20ºC to 100ºC and computing the slope of the linear regression derived from the measurements. Fig. 4 shows the TCF measurements for longitudinal mode SMRs and fig. 5 shows the TCF measurements for shear mode devices.

Ranging from -25.27 to -16.91 ppm/ºC, the outcome of these measurements lay on the same region as the rest of conventional AlN-based devices, meaning that substituting more common high impedance materials with ZnO does not induce extra deviation in the behavior of frequency response variations due to temperature changes. Therefore, similar steps to the ones carried out to similar devices could successfully achieve temperature compensation.

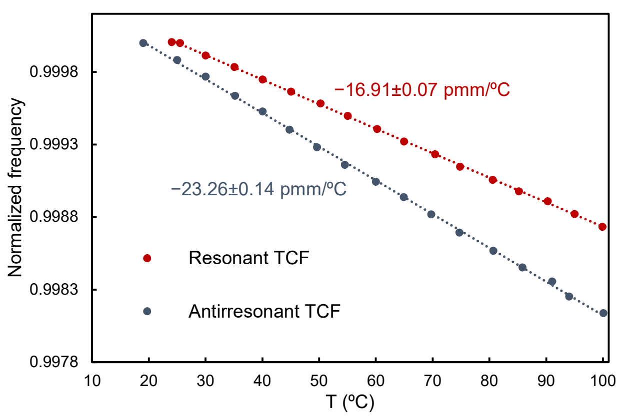

Fig. 4. TCF measurements for longitudinal mode.

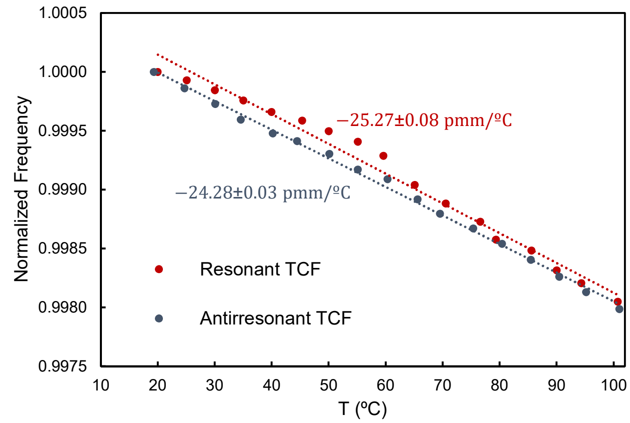

Fig. 5. TCF measurements for shear mode.

IV. CONCLUSIONS

In this work we observe how an acoustic reflector with ZnO working as high impedance material maintains its acoustic performance after being exposed to a 700ºC temperature treatment, showing its good thermal stability. Regarding Q values, they show that no extra source of acoustic energy loss is introduced, meaning that the acoustic reflectors preserve their properties and structure, and providing good acoustic insulation. TCF measurements also show that variation of frequency with temperature has a similar behavior compared to AlN-based SMRs fabricated on top of other common acoustic reflectors. This could mean not only that devices built with this configuration can perform in these temperature ranges, but that they can potentially keep this performance after being exposed to extra fabrication steps, for instance, to work as gravimetric sensors.

AKNOWLEDGMENT

This work was funded by project PID-2020-118410RB-C22 of the R&D National Plan of Spanish Government.

REFERENCES

[1] K. Hashimoto, *RF Bulk Acoustic Wave Filters for Communications*. Artech House, 2009.

[2] R. Aigner *et al.*, "Bulk-acoustic-wave filters: Performance optimization and volume manufacturing," in *IEEE MTT-S International Microwave Symposium Digest*, 2003, vol. 3, pp. 2001–2004.

[3] J. Olivares, E. Wegmann, M. Clement, J. Capilla, E. Iborra, and J. Sangrador, "Wide bandwidth Bragg mirrors for multi-band filter chips," *Proc. - IEEE Ultrason. Symp.*, pp. 2119–2122, 2009.

[4] C. J. Chung, Y. C. Chen, C. C. Cheng, and K. S. Kao, "Fabrication and frequency response of solidly mounted resonators with 1/4λ mode configuration," *Thin Solid Films*, vol. 516, no. 16, pp. 5277–5281, 2008.

[5] A. Reinhardt *et al.*, "Simulation of BAW resonators frequency adjustment," in *Proceedings - IEEE Ultrasonics Symposium*, 2007, pp. 1444–1447.

[6] J. Capilla, J. Olivares, M. Clement, J. Sangrador, E. Iborra, and A. Devos, "High-acoustic-impedance tantalum oxide layers for insulating acoustic reflectors," *IEEE Trans. Ultrason. Ferroelectr. Freq. Control*, vol. 59, no. 3, pp. 366–372, 2012.

[7] C. W. Seabury, "United States Patent (19)," 1992.

[8] J. M. Carmona-Cejas, T. Mirea, M. Clement, and J. Olivares, "Comparative study of fully-dielectric acoustic reflectors in solidly mounted resonators," in *IEEE Intern. Ultras. Symposium, IUS*, 2021.